

Protein-mimicking nanoparticle (Protmin)-based nanosensor for intracellular analysis of metal ions

Dan Zhu^{1,2} · Dong-Xia Zhao² · Jia-Xuan Huang² · Jiang Li¹ · Xiao-Lei Zuo¹ · Li-Hua Wang¹ · Chun-Hai Fan¹

Received: 7 June 2017/Revised: 17 September 2017/Accepted: 22 September 2017/Published online: 21 December 2017
© Shanghai Institute of Applied Physics, Chinese Academy of Sciences, Chinese Nuclear Society, Science Press China and Springer Nature Singapore Pte Ltd. 2017

Abstract In this study, we designed and applied protein-mimicking nanoparticles (Protmin) as an intracellular nanosensor for in vivo detection of lead ions (Pb^{2+}). Monodispersed gold nanoparticles (AuNPs) of 13 nm in diameter were modified using poly-adenine-tailed Pb^{2+} -specific 8–17 DNAzyme to form a spherical and functional Protmin. Substrate strands modified with a fluorophore at the 5' end and a quencher at the 3' end were bound to DNAzyme. Pb^{2+} facilitated cleavage of DNAzyme to release the fluorophore-modified short strands to generate fluorescence. We observed rapid kinetics of the Protmin nanosensor, for which the typical assay time was 10 min. Further, we demonstrated the Protmin nanosensor could readily enter living cells and respond to Pb^{2+} in the intracellular environment. The broad range of Protmin

designs will be useful for advancing biological and medical applications.

Keywords Protmin · Nanosensor · Poly-adenine · Lead ion · Intracellular detection

1 Introduction

Metal ions play an important role in cellular activities and participate in a variety of physiological processes. The maintenance of proper concentrations of metal ions in cells or tissues fundamentally affects various processes, such as supporting the basic structures and functions of nucleic acids, proteins, and hormones [1–3]. Recent studies demonstrated that various diseases, such as neural disturbance, organic damage, and cancer or gene mutation, are related to abnormal levels of metal ions or the presence of toxic metal ions [4–6]. Over the past few decades, many sensors have been designed to detect metal ions in environmental samples or biological samples with a high sensitivity and selectivity [7–12]. In recent years, tracing metal ions in cells have generated concerns because of their fundamental roles in biology and health. Developing sensitive, fast, and responsive cellular sensors is very important for understanding different functions at the molecular level in cells.

Proteins are among the most important components in cells and tissues in the body and participate in various physiological processes. Proteins also have a significant clinical value in disease diagnosis and as therapeutics [13]. Therefore, developing proteins with specific functions has been widely examined. However, natural proteins regulate their catalytic activity by binding to scaffolding proteins or

This work was supported by the National Natural Science Foundation of China (Nos. 21390414 and 21605087), the Chinese Academy of Sciences (No. QYZDJ-SSW-SLH031), the China Postdoctoral Science Foundation funded project (No. BX201700123), the Scientific Research Foundation of Nanjing University of Posts and Telecommunications (No. NY215058), and the Natural Science Fund for Colleges and Universities in Jiangsu Province (16KJB150032).

✉ Chun-Hai Fan
fchh@sinap.ac.cn

¹ Division of Physical Biology and Bioimaging Center, Shanghai Synchrotron Radiation Facility, Shanghai Institute of Applied Physics, Chinese Academy of Sciences, Shanghai 201800, China

² Key Laboratory for Organic Electronics and Information Displays, Institute of Advanced Materials (IAM), Jiangsu National Synergetic Innovation Center for Advanced Materials (SICAM), Jiangsu Key Laboratory for Biosensor, Nanjing University of Posts and Telecommunications, Nanjing 210023, China

assembling at the membrane and do not effectively cross the membrane of cells to exert their functions. Thus, the utilization of proteins as diagnostic probes and therapeutic agents is limited because of their instability and poor transduction across cell membranes. Nanomaterials may be useful for overcoming these limitations. By combining nanomaterials with enzyme-like molecules, protein-mimicking nanoparticles (Protmins) can be developed with multiple functions and favorable stability in the biological environment. Gold nanoparticles (AuNPs) have been widely investigated nanomaterials because of their unique chemical and physical properties. The high surface-to-volume ratio, favorable chemical stability, and easy modification make AuNPs applicable for biosensing [14–17], nanophotonics [18, 19], catalysis [20–22], and drug delivery [23–25]. Through assembly with DNA probes, AuNP conjugates can enter cells without the use of additional transfection agents [26], enabling the construction of protein-mimicking nanostructures with excellent biocompatibility.

In this study, we constructed and applied an AuNP-based Protmin as an intracellular nanosensor for efficient *in vivo* lead (Pb^{2+}) detection. DNAzyme was employed as a recognition and sensing element in the design of Protmin. As an enzyme-like oligonucleotide, DNAzyme can efficiently recognize its specific target with excellent specificity and possesses catalytic proteinase-like activity [27, 28]. DNAzyme assembled onto AuNPs efficiently recognized intracellular target metal ions, such as uranyl [29], copper, and zinc ions [30]. Salaita et al. evaluated the activity of DNAzyme on AuNPs and found that it mostly depended on the conformation and density of DNAzyme on the nanointerface, while the active sites of DNAzyme might be hidden by the adsorption between DNA and the gold surface [31]. To improve the activity of Protmin, a poly-adenine (polyA)-tailed probe was employed, which has been shown to have high activity *in vitro* [32–36]. The polyA tail serves as an efficient anchoring block based on its preferential binding with the AuNP surface and prevents nonspecific adsorption between the active sites of DNAzyme and gold surface, thus improving the sensitivity for Pb^{2+} detection. The sensitivity, selectivity, and kinetics of the Protmin-based nanosensor were investigated *in vitro*. The existence of intracellular Pb^{2+} was evaluated by fluorescence imaging, which was an effective tool for investigating subcellular structures and intracellular fluorescence [19]. By transferring this Protmin nanosensor into cells, intracellular toxic Pb^{2+} can be detected.

2 Experimental section

2.1 Apparatus and materials

Oligonucleotides (Table 1) were synthesized and purified by TaKaRa, Inc. (Shiga, Japan). $\text{HAuCl}_4 \cdot 4\text{H}_2\text{O}$ (99.9%), NaCl, $\text{NaH}_2\text{PO}_4 \cdot 2\text{H}_2\text{O}$, and $\text{NaH}_2\text{PO}_4 \cdot 12\text{H}_2\text{O}$ were purchased from China National Pharmaceutical Group Corporation (Shanghai, China). $\text{Pb}(\text{OAc})_2$, 6-mercapto-1-hexanol (MCH), diethylpyrocarbonate (DEPC), trisodium citrate, ethyl acetate, and other chemicals were all obtained from Sigma-Aldrich (St. Louis, MO, USA). All solutions were prepared with ultrapure water (18.2 M Ω cm). Transmission electron microscopy (TEM) imaging was performed using H-7500 model (Hitachi, Tokyo, Japan). UV–Vis spectra were measured with a U-3900 (Hitachi). Fluorescence measurements were performed on an F-4500 (Hitachi). Cell imaging and fluorescence imaging in cells were conducted using a laser confocal microscope (Leica TCS SP5, Wetzlar, Germany).

2.2 Preparation of 13-nm AuNPs

Thirteen-nanometer AuNPs were synthesized following classical citrate reduction procedures [37]. Briefly, 3.5 mL of 1% trisodium citrate was quickly added to a boiling, rapidly stirring 0.01% aqueous HAuCl_4 solution, which changed the solution color from pale yellow to burgundy red. After further boiling for 20 min, the solution was left to cool to 25 °C while stirring. The prepared AuNPs were stored at 4 °C until use, and the size of the AuNPs was determined by TEM imaging.

2.3 Preparation of polyA-tailed Protmin

The prepared AuNPs were first incubated with polyA-tailed DNAzyme (polyA10-17E) in a 1:200 ratio for 16 h. Next, 1 M of phosphate-buffered saline (PBS, 1 M of NaCl, 100 mM of $\text{NaH}_2\text{PO}_4/\text{Na}_2\text{HPO}_4$, pH 7.4) was added to the mixture 5 times repeatedly at 30-min intervals to achieve a 0.1 M phosphate concentration. The salt solution was incubated for an additional 40 h at room temperature. Next, the solution was centrifuged (13,500 rpm, 20 min) and resuspended in 0.1 M PBS (0.1 M of NaCl, 10 mM of $\text{NaH}_2\text{PO}_4/\text{Na}_2\text{HPO}_4$, pH 7.4) three times. The prepared Protmin was resuspended in the reaction buffer (20 mM tris, 100 mM NaCl, pH 7.4, prepared in DEPC-treated water) until use.

Table 1 Base sequences and their labeling of DNA oligonucleotide samples used in the study

DNA name	sequence (5'–3')
polyA10-17E	AAAAAAAAAATTTTTCATCTCTTCTCCGAGCCGGTTCGAAATAGTGAGT
polyA10-17E-F	AAAAAAAAAATTTTTCATCTCTTCTCCGAGCCGGTTCGAAATAGTGAGT-FAM
Active 17S	Cy3-ACTCACTATrAGGAAGAGATG-BHQ-2
Inactive 17S	Cy3-ACTCACTATAGGAAGAGATG-BHQ-2

2.4 Calculation of 17E loading on AuNPs

The loading of 17E was determined by attaching FAM-labeled 17E (polyA10-17E-F) onto the 13-nm AuNPs. The concentration of 17E-AuNPs was determined by UV–Vis spectroscopy measurements using Beer's law (for 13-nm AuNPs, $\epsilon_{520\text{ nm}} = 2.7 \times 10^8 \text{ L mol}^{-1} \text{ cm}^{-1}$). FAM-labeled 17E was chemically displaced from the surface of AuNPs by MCH treatment (final concentration 10 mM in 0.3 M NaCl, 10 mM phosphate buffer solution, pH 7.4) after 18-h incubation at 37 °C with shaking. The released fluorescent DNA was collected via centrifugation and measured with the F-4500. The fluorescence was converted to molar concentrations of probes by comparison with a standard curve, which was prepared using known concentrations of 17E-F under the same conditions. The loading of DNA was calculated by dividing the concentration of fluorescent 17E-F by the concentration of AuNPs. Experiments were repeated three times using fresh samples.

2.5 Determination of activity of Protmin nanosensor in vitro

The RNA contained substrate strand “Active 17S” was modified with Cy3 label at the 5' end and BHQ-2 at the 3' end. The Protmin nanosensor was fabricated as follows. First, active 17S was added to a Protmin solution to a final ratio of 2:1 17S to 17E strand. The solution was heated at 65 °C for 5 min and then cooled at 25 °C for 1 h. The solution was stored at 4 °C overnight to complete the reaction. Excess 17S was removed by centrifugation and the prepared Protmin nanosensor was washed with reaction buffer three times. Finally, the Protmin nanosensor was diluted to a concentration of 2 nM in the reaction buffer. A series concentration of $\text{Pb}(\text{OAc})_2$ stock solution was added to the Protmin nanosensor. Fluorescence spectra were collected at 540-nm excitation.

2.6 Pb^{2+} cellular uptake and imaging

Active or inactive Protmin nanosensors were prepared by hybridizing “Active 17S” or “Inactive 17S” with Protmin. HeLa cells were dispersed at a density of 1.0×10^5 cells per well in 24-well microtiter plates to a total volume of 500 μL /well. The plates were maintained at

37 °C in a 5% $\text{CO}_2/95\%$ air incubator for 1 day. After removing the original incubation medium, HeLa cells were incubated with Pb^{2+} at a final concentration of 200 μM for 12 h to allow sufficient metal ion uptake. The cells were washed thrice using 0.1 M PBS. Next, 600 μL of Dulbecco's modified Eagle medium (DMEM) culture medium containing 2 nM active or inactive A10-17ES-AuNPs was added. After 2 h of incubation, the cells were washed using PBS thrice and fresh DMEM was added. Lysotracker Green was added to the cells for another 30 min at a final concentration of 50 nM. Fluorescence images were acquired with a confocal laser scanning microscope.

2.7 MTT assay

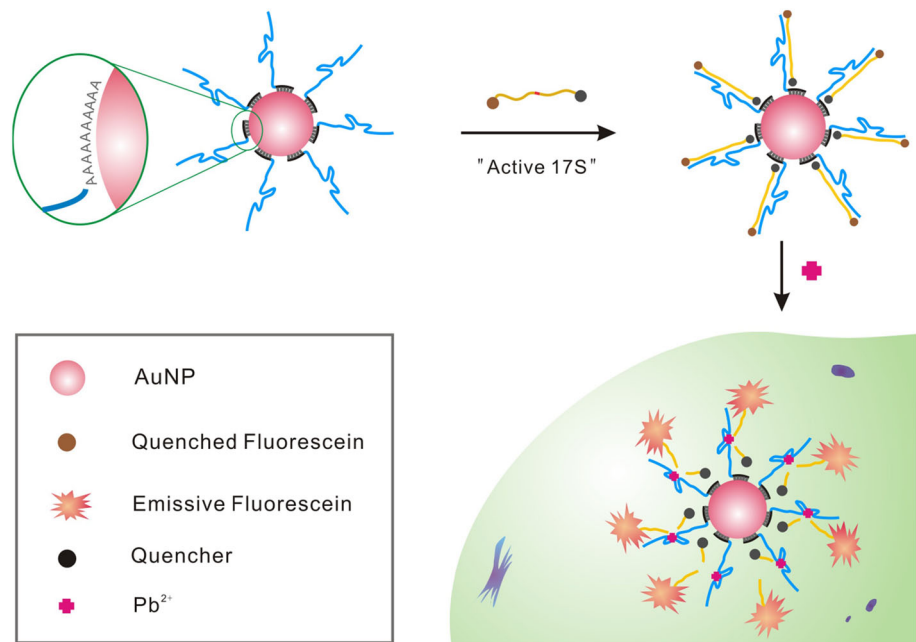
An MTT assay was carried out to investigate the cytotoxicity of the nanosensor. HeLa cells (1.0×10^5 cells per well) were dispersed in 24-well microtiter plates to a total volume of 500 μL /well. The plates were maintained at 37 °C in a 5% $\text{CO}_2/95\%$ air incubator for 1 day. After removing the original medium, HeLa cells were incubated with unmodified AuNPs (1 nM) or nanosensor (1 nM and 3 nM) for 3, 6, 12, and 24 h. Next, the medium was replaced with another medium containing MTT (0.5 mg/mL) and cells were incubated for another 4-h incubation at 37 °C. After removing the medium, 150 μL DMSO was added to the cells to dissolve the formed formazan. Absorbance at 490 nm in each well was recorded. Cell viability was expressed as the ratio of the absorbance of the cells incubated with AuNPs or the nanosensor to that of cells incubated with only culture medium.

3 Results and discussion

3.1 Fabrication and working principle of the Protmin nanoprobe

Based on the polyA-tailed DNAzyme specific for Pb^{2+} cleavage, we constructed a Protmin nanosensor for Pb^{2+} detection in cells. As shown in Fig. 1, Protmin was first prepared by attaching the polyA-tailed DNAzyme onto the surface of AuNPs through polyA-Au binding, extending the DNAzyme block for further reactions. Protmin was then hybridized with the fluorescent 17S substrate strands

Fig. 1 (Color online) Schematic illustration of Pb^{2+} imaging in living cells based on polyA-tailed protein-mimicking nanoparticles (Protmin)



to fabricate 17ES-AuNP. The substrate strands were labeled with a fluorophore at the 5' end and quencher at the 3' end. After attachment to the AuNPs, the fluorophore was quenched by gold and a quencher, resulting in very weak fluorescence. In the presence of Pb^{2+} , the substrate strands were cleaved, resulting in the release of short fluorophore-labeled DNA and an increase in fluorescence.

3.2 Characterization of Protmin probe

Because the 13-nm AuNP was reported to be an efficient quencher [38] and intracellular nanocarrier [26], our design was based on this intracellular nanosensor. TEM images of AuNPs (Fig. 2a) showed that the 13-nm AuNPs were successfully synthesized with good dispersion. The UV-Vis absorption spectra of AuNPs and polyA10-tailed Protmin (AuNPs functionalized with polyA10-tailed DNAzyme)

shown in Fig. 2b demonstrated that the maximum optical absorption was shifted from 520 to 524 nm after polyA-tailed DNAzyme assembly on the surface of AuNPs. Because the position of the plasmon band of metal nanoparticles was closely related to the size and surrounding environment, the red shift in spectroscopy confirmed that the AuNPs were successfully functionalized with polyA10-tailed DNAzyme [39]. By using a displacement-based fluorescence method established by Mirkin [40], each AuNP was estimated to carry 42 ± 2 DNAzyme, which was in accordance with our previous result [33].

3.3 Pb^{2+} detection of Protmin nanosensor in vitro

We first evaluated the feasibility of using the Protmin nanosensor for Pb^{2+} detection in vitro (Fig. 3a). The curve a in Fig. 3a shows the fluorescence spectrum of free Cy3-

Fig. 2 (Color online) **a** TEM images of 13-nm AuNPs; **b** UV-Vis spectra for unmodified AuNPs (black line) and the Protmin (red line)

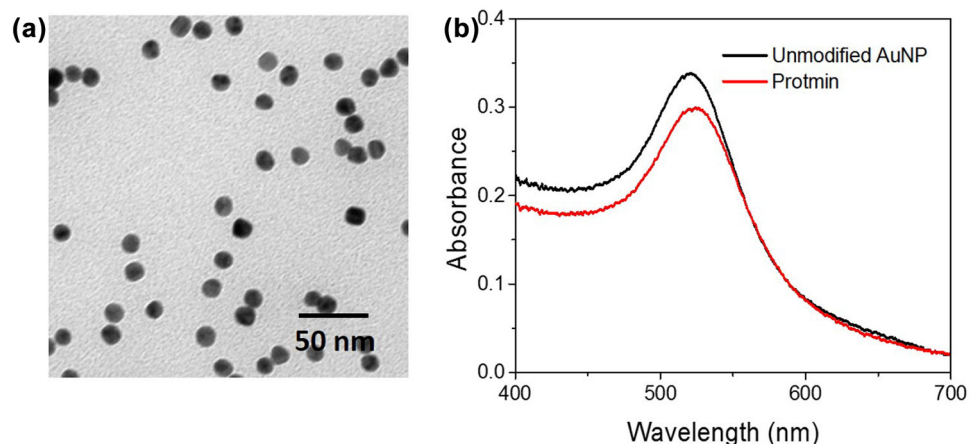
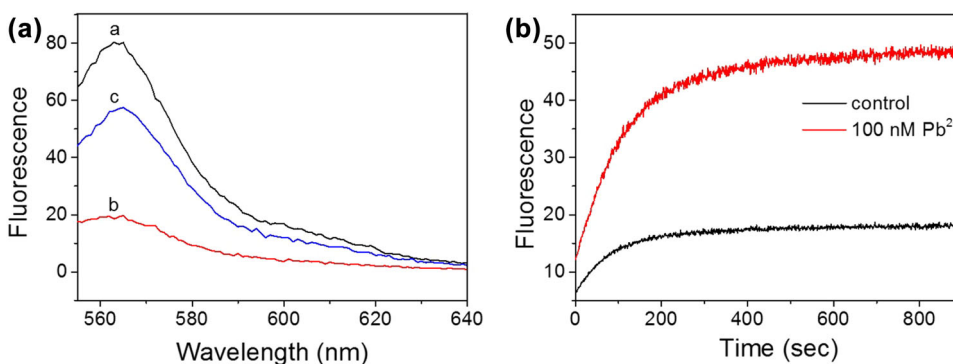


Fig. 3 (Color online) **a** Fluorescence spectra of Cy3- and BHQ-2-labeled “Active 17S” in solution (curve *a*), Protmin-based nanosensor in the absence (curve *b*) and presence (curve *c*) of 100 nM Pb²⁺; **b** kinetics of the nanoprobe in the absence (black curve) and presence of 100 nM Pb²⁺. The excitation wavelength was 540 nm



and BHQ-2-labeled active 17E solution upon excitation at 540 nm. After hybridization with Protmin, fluorescence was decreased significantly because of efficient quenching by AuNPs (curve *b* in Fig. 3a). After adding Pb²⁺, the substrate strand was cleaved and the Cy3-labeled short strand was released, increasing the fluorescence of the system (curve *c* in Fig. 3a). These results indicated that the Protmin nanosensor functioned well in response to Pb²⁺ in vitro. The results of kinetics in Fig. 3b showed that the Protmin nanosensor responded rapidly to Pb²⁺ and the fluorescence at 565 nm reached a plateau after 10-min incubation with Pb²⁺, which was twofold faster than that of a thiolated DNAzyme-based nanosensor [29]. These fast kinetic results may be attributed to the elimination of nonspecific adsorption between gold and DNAzyme by using polyA tails. These results demonstrate the potential for rapid detection by using Protmin-based sensors.

3.4 Sensitivity of selectivity of Protmin nanosensor in vitro

To test the sensitivity of the nanosensor, different concentrations of Pb²⁺ (0–2 μM) were added and emission fluorescence was recorded. The fluorescence signal at

565 nm increased as the concentration of Pb²⁺ increased (Fig. 4a). Good linearity was obtained from 5–30 nM. The linear equation was fluorescence ($F_{565\text{ nm}}$) = 0.6732 $C_{\text{Pb}^{2+}}$ (nM) + 21.66, with a correlation coefficient of 0.9143.

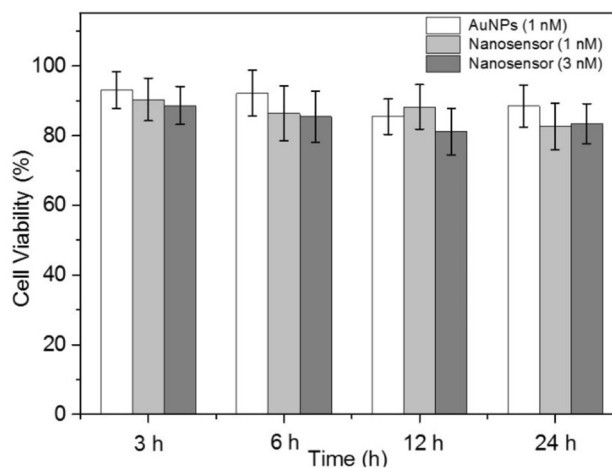


Fig. 5 MTT assay of HeLa cells. HeLa cells were incubated with unmodified AuNPs (1 nM), nanosensor (1 and 3 nM) for 3, 6, 12, and 24 h. Error bars represent variations between three parallel experiments

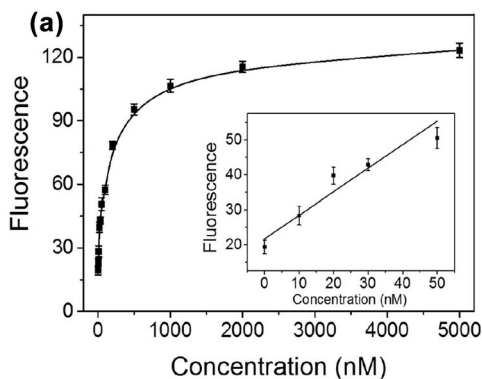
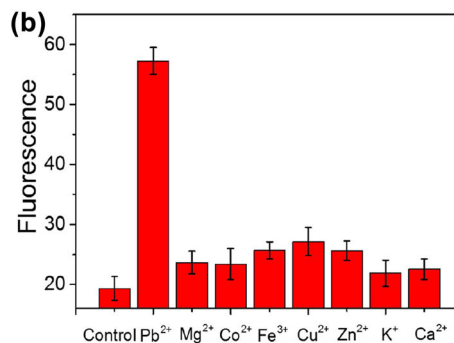


Fig. 4 (Color online) **a** Fluorescence intensity at 565 nm in the presence of various concentrations of Pb²⁺ (0, 5, 10, 15, 20, 30, 50, 100, 200, 500, 1000, and 2000 nM). Inset: Calibration curve for the fluorescence intensity versus corresponding Pb²⁺ concentration.



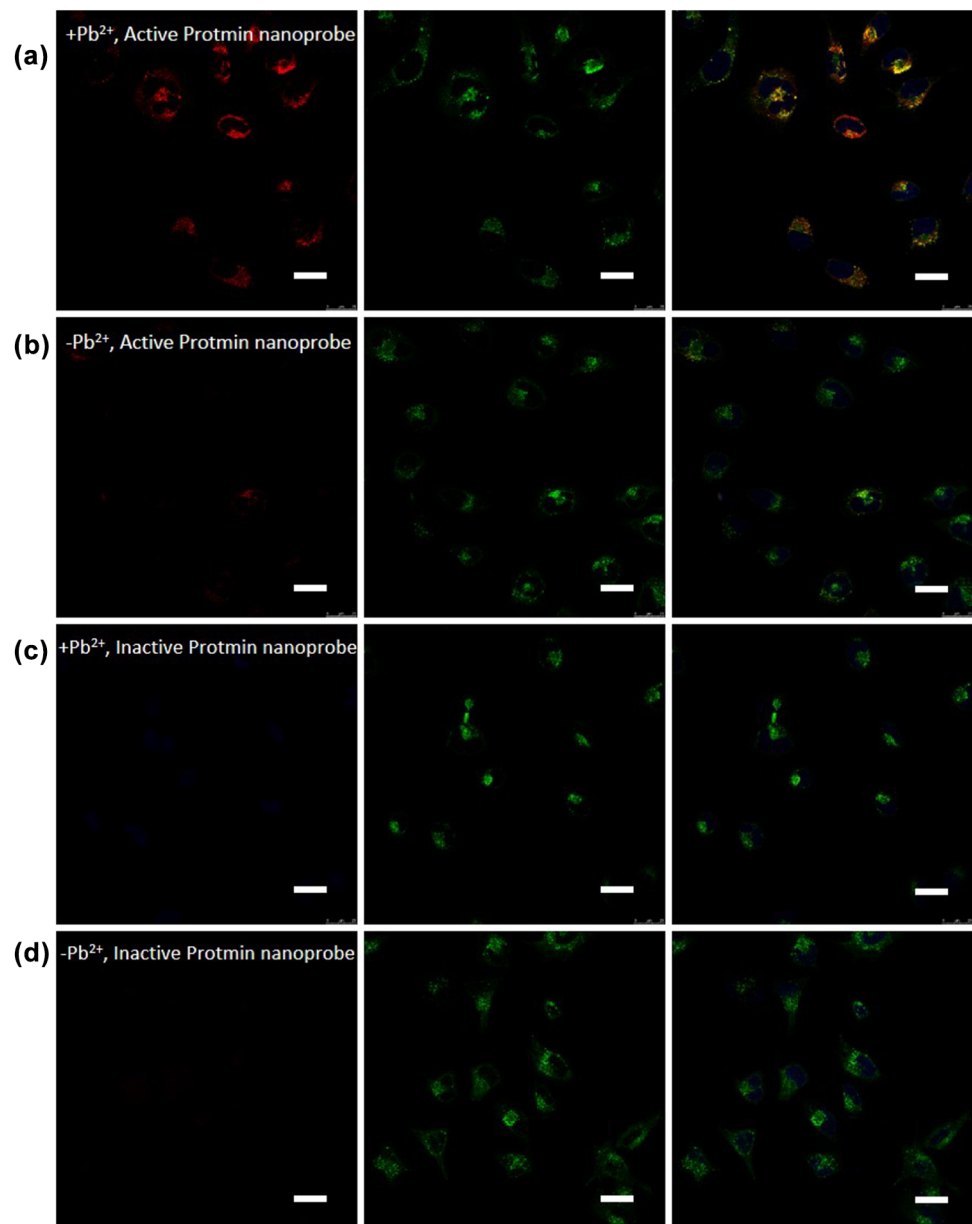
b Specificity of the nanoprobe for Pb²⁺ compared to other metal ions (Mg²⁺, Co²⁺, Fe³⁺, Cu²⁺, Zn²⁺, K⁺, Ca²⁺). The concentration of other metal ions was 50 μM and concentration of Pb²⁺ was 100 nM. The excitation wavelength was 540 nm

The detection limit of Pb^{2+} was calculated to be 5.33 nM. This assay is more sensitive or comparable to other intracellular Pb^{2+} assays [41–43] because of the high activity of polyA-mediated DNAzyme on AuNPs [33]. To evaluate the selectivity of the nanoprobe for sensing Pb^{2+} , other biologically relevant metal ions, including Mg^{2+} , Co^{2+} , Fe^{3+} , Cu^{2+} , Zn^{2+} , K^+ , and Ca^{2+} , were tested. As shown in Fig. 4b, the Protmin nanosensor exhibited two- to threefold higher fluorescence signals for Pb^{2+} than for other metal ions at higher concentrations. Thus, the nanosensor is suitable for evaluation in complex biological systems.

3.5 Intracellular sensing of Pb^{2+} using Protmin nanosensor

The application of the Protmin-based nanosensor for intracellular Pb^{2+} was tested. The cellular uptake and fluorescence response of the sensor were evaluated using HeLa cells as a model. To evaluate the cytotoxicity of the nanosensor, an MTT (3-(4,5-dimethylthiazol-2-yl)-2,5-diphenyltetrazolium bromide) assay in HeLa cells was performed. The results indicated that the AuNPs (1 nM) and nanosensor (1 and 3 nM) showed low cytotoxicity or side effects in HeLa cells (Fig. 5). Therefore, the

Fig. 6 (Color online) **a**, **b** Confocal microscopy images of HeLa cells treated **a** with or **b** without Pb^{2+} with active Protmin nanosensor. **c**, **d** Confocal microscopy images of HeLa cells treated **a** with or **b** without Pb^{2+} with inactive Protmin nanosensor. The red channel is Cy3 fluorescence and green channel is LysoTracker Green fluorescence. The scale bar is 25 μm



nanosensor is a reliable probe for detection in biological samples.

We first treated HeLa cells with 200 μM Pb^{2+} for 12 h to allow sufficient metal ion uptake. According to a previous study [29], the AuNP-DNAzyme nanoprobe can enter cells through receptor-mediated endocytosis without the use of transfection agents. As shown in Fig. 6a, a red fluorescence signal corresponding to Pb^{2+} was observed. As a control, HeLa cells without treated with Pb^{2+} were also incubated with the nanoprobe and imaged under the same conditions and nearly no fluorescence signal was observed (Fig. 6b). To further confirm that the fluorescence observed in Fig. 6a was because of the activity of DNAzyme, an inactive Protmin nanosensor was prepared by using “Inactive 17S,” in which the adenosine ribonucleotide at the cleavage site was replaced with a deoxyribonucleotide. As shown in Fig. 6c, d, the inactive probe-treated HeLa cells showed less fluorescence than those with the active probe. Staining of lysosomes of cells (green) showed good colocalization of LysoTracker and Protmin nanoprobe, indicating that the nanoprobe was mainly transported to the lysosomes. These results are consistent with those for other nanoprobe constructed based on DNA-AuNPs [29, 30]. The results demonstrated the successful implementation of intracellular detection of Pb^{2+} by using this Protmin nanoprobe.

4 Conclusion

In summary, we developed a novel intracellular nanosensor based on high-efficient polyA-tailed Protmin with fast kinetics for Pb^{2+} detection in HeLa cells. Protmin not only possesses enzyme-like catalysis activity, but also has advantages of nanomaterials, such as excellent chemical stability and unique chemistry and it is easy to transduce across cell membranes. Additionally, the polyA tail added to Protmin decreased nonspecific adsorption between DNA and gold, thus enhancing the activity of DNAzyme at the nanointerface. PolyA contains natural nucleotides that are easy to synthesize and modify, and thus reduces synthesis costs. Fast kinetics of the Protmin nanosensor were observed and the detection time in vitro was decreased to 10 min, indicating that this system can be used for a rapid detection. In combination with DNAzyme specific for other metal ions, the polyA-tailed Protmin nanoprobe is a simple and general platform for developing high-efficient intracellular nanosensors. The Protmin design is promising for constructing nanostructures mimicking protein functions, which may have wide applications in biomedicine and life sciences.

References

1. A.M. Pyle, Metal ions in the structure and function of RNA. *J. Biol. Inorg. Chem.* **7**, 679–690 (2002). <https://doi.org/10.1007/s00775-002-0387-6>
2. C.A. Blindauer, O.I. Leszczyszyn, Metallothioneins: unparalleled diversity in structures and functions for metal ion homeostasis and more. *Nat. Prod. Rep.* **27**, 720–741 (2010). <https://doi.org/10.1039/b906685n>
3. A. Rolfs, M.A. Hediger, Metal ion transporters in mammals: structure, function and pathological implications. *J. Physiol. Lond.* **518**, 1–12 (1999). <https://doi.org/10.1111/j.1469-7793.1999.0001r.x>
4. P.G. Georgopoulos, A. Roy, M.J. Yonone-Lioy et al., Environmental copper: its dynamics and human exposure issues. *J. Toxicol. Env. Health B* **4**, 341–394 (2001). <https://doi.org/10.1080/109374001753146207>
5. A.T. Jan, M. Azam, K. Siddiqui et al., Heavy metals and human health: mechanistic insight into toxicity and counter defense system of antioxidants. *Int. J. Mol. Sci.* **16**, 29592–29630 (2015). <https://doi.org/10.3390/ijms161226183>
6. S.C. Izah, N. Chakrabarty, A.L. Srivastav, A review on heavy metal concentration in potable water sources in Nigeria: human health effects and mitigating measures. *Expos. Health* **8**, 285–304 (2016). <https://doi.org/10.1007/s12403-016-0195-9>
7. G. Liang, Y. Man, A. Li et al., DNAzyme-based biosensor for detection of lead ion: a review. *Microchem. J.* **131**, 145–153 (2017). <https://doi.org/10.1016/j.microc.2016.12.010>
8. D. Li, S. Song, C. Fan, Target-responsive structural switching for nucleic acid-based sensors. *Acc. Chem. Res.* **43**, 631–641 (2010). <https://doi.org/10.1021/ar900245u>
9. X. Qu, F. Yang, H. Chen et al., Bubble-mediated ultrasensitive multiplex detection of metal ions in three-dimensional DNA nanostructure-encoded microchannels. *ACS Appl. Mater. Inter.* **9**, 16026–16034 (2017). <https://doi.org/10.1021/acsami.7b03645f>
10. S. He, D. Li, C. Zhu et al., Design of a gold nanoprobe for rapid and portable mercury detection with the naked eye. *Chem. Commun.* (2008). <https://doi.org/10.1039/b811528a>
11. L. Li, Y. Wen, L. Xu et al., Development of mercury (II) ion biosensors based on mercury-specific oligonucleotide probes. *Biosens. Bioelectron.* **75**, 433–445 (2016). <https://doi.org/10.1016/j.bios.2015.09.003>
12. J. Wu, L. Li, D. Zhu et al., Colorimetric assay for mercury (II) based on mercury-specific deoxyribonucleic acid-functionalized gold nanoparticles. *Anal. Chim. Acta* **694**, 115–119 (2011). <https://doi.org/10.1016/j.aca.2011.02.045>
13. S.B. Fonseca, M.P. Pereira, S.O. Kelley, Recent advances in the use of cell-penetrating peptides for medical and biological applications. *Adv. Drug Deliver. Rev.* **61**, 953–964 (2009). <https://doi.org/10.1016/j.addr.2009.06.001>
14. M.C. Daniel, D. Astruc, Gold nanoparticles: assembly, supramolecular chemistry, quantum-size-related properties, and applications toward biology, catalysis, and nanotechnology. *Chem. Rev.* **104**, 293–346 (2004). <https://doi.org/10.1021/cr030698+>
15. K. Saha, S.S. Agasti, C. Kim et al., Gold nanoparticles in chemical and biological sensing. *Chem. Rev.* **112**, 2739–2779 (2012). <https://doi.org/10.1021/cr2001178>
16. S. Su, X. Zuo, D. Pan et al., Design and applications of gold nanoparticle conjugates by exploiting biomolecule-gold nanoparticle interactions. *Nanoscale* **5**, 2589–2599 (2013). <https://doi.org/10.1039/c3nr33870c>
17. P. Chen, D. Pan, C. Fan et al., Gold nanoparticles for high-throughput genotyping of long-range haplotypes. *Nat.*

- Nanotechnol. **6**, 639–644 (2011). <https://doi.org/10.1038/nnano.2011.141>
18. A.N. Yakunin, Y.A. Avetisyan, V.V. Tuchin, Quantification of laser local hyperthermia induced by gold plasmonic nanoparticles. *J. Biomed. Opt.* (2015). <https://doi.org/10.1117/1.jbo.20.5.051030>
 19. S. Wang, S. Deng, X. Cai et al., Superresolution imaging of telomeres with continuous wave stimulated emission depletion (STED) microscope. *Sci. China Chem.* **59**, 1519–1524 (2016). <https://doi.org/10.1007/s11426-016-0020-9>
 20. A. Corma, H. Garcia, Supported gold nanoparticles as catalysts for organic reactions. *Chem. Soc. Rev.* **37**, 2096–2126 (2008). <https://doi.org/10.1039/b707314n>
 21. X. Zheng, Q. Liu, C. Jing et al., Catalytic gold nanoparticles for nanoplasmonic detection of DNA hybridization. *Angew. Chem. Inter. Ed.* **50**, 11994–11998 (2011). <https://doi.org/10.1002/anie.201105121>
 22. K. Li, K. Wang, W. Qin et al., DNA-directed assembly of gold nanohalo for quantitative plasmonic imaging of single-particle catalysis. *J. Am. Chem. Soc.* **137**, 4292–4295 (2015). <https://doi.org/10.1021/jacs.5b00324>
 23. E. Boisselier, D. Astruc, Gold nanoparticles in nanomedicine: preparations, imaging, diagnostics, therapies and toxicity. *Chem. Soc. Rev.* **38**, 1759–1782 (2009). <https://doi.org/10.1039/b806051g>
 24. E.C. Dreaden, A.M. Alkilany, X. Huang et al., The golden age: gold nanoparticles for biomedicine. *Chem. Soc. Rev.* **41**, 2740–2779 (2012). <https://doi.org/10.1039/c1cs15237h>
 25. P. Ghosh, G. Han, M. De et al., Gold nanoparticles in delivery applications. *Adv. Drug Deliver. Rev.* **60**, 1307–1315 (2008). <https://doi.org/10.1016/j.addr.2008.03.016>
 26. N.L. Rosi, D.A. Giljohann, C.S. Thaxton et al., Oligonucleotide-modified gold nanoparticles for intracellular gene regulation. *Science* **312**, 1027–1030 (2006). <https://doi.org/10.1126/science.1125559>
 27. L. Lermer, Y. Roupiez, R. Ting et al., Toward an RNaseA mimic: a DNzyme with imidazoles and cationic amines. *J. Am. Chem. Soc.* **124**, 9960–9961 (2002). <https://doi.org/10.1021/ja0205075>
 28. Y.F. Li, D. Sen, Toward an efficient DNzyme. *Biochemistry* **36**, 5589–5599 (1997). <https://doi.org/10.1021/bi962694n>
 29. P. Wu, K. Hwang, T. Lan et al., A DNzyme-gold nanoparticle probe for uranyl ion in living cells. *J. Am. Chem. Soc.* **135**, 5254–5257 (2013). <https://doi.org/10.1021/ja400150v>
 30. L. Li, J. Feng, Y. Fan et al., Simultaneous imaging of Zn²⁺ and Cu²⁺ in living cells based on DNzyme modified gold nanoparticle. *Anal. Chem.* **87**, 4829–4835 (2015). <https://doi.org/10.1021/acs.analchem.5b00204>
 31. K. Yehl, J.R. Joshi, B.L. Greene et al., Catalytic deoxyribozyme-modified nanoparticles for RNAi-independent gene regulation. *ACS Nano* **6**, 9150–9157 (2012). <https://doi.org/10.1021/nm3034265>
 32. H. Pei, F. Li, Y. Wan et al., Designed diblock oligonucleotide for the synthesis of spatially isolated and highly hybridizable functionalization of DNA-gold nanoparticle nanoconjugates. *J. Am. Chem. Soc.* **134**, 11876–11879 (2012). <https://doi.org/10.1021/ja304118z>
 33. D. Zhu, H. Pei, J. Chao et al., Poly-adenine-based programmable engineering of gold nanoparticles for highly regulated spherical DNzymes. *Nanoscale* **7**, 18671–18676 (2015). <https://doi.org/10.1039/c5nr05366h>
 34. G. Yao, H. Pei, J. Li et al., Clicking DNA to gold nanoparticles: poly-adenine-mediated formation of monovalent DNA-gold nanoparticle conjugates with nearly quantitative yield. *NPG Asia Mater.* (2015). <https://doi.org/10.1038/am.2014.131>
 35. D. Zhu, J. Chao, H. Pei et al., Coordination-mediated programmable assembly of unmodified oligonucleotides on plasmonic silver nanoparticles. *ACS Appl. Mater. Inter.* **7**, 11047–11052 (2015). <https://doi.org/10.1021/acsami.5b03066>
 36. D. Zhu, P. Song, J. Shen et al., PolyA-mediated DNA assembly on gold nanoparticles for thermodynamically favorable and rapid hybridization analysis. *Anal. Chem.* **88**, 4949–4954 (2016). <https://doi.org/10.1021/acs.analchem.6b00891>
 37. K.C. Grabar, R.G. Freeman, M.B. Hommer et al., Preparation and characterization of Au colloid monolayers. *Anal. Chem.* **67**, 735–743 (1995). <https://doi.org/10.1021/ac00100a008>
 38. B. Dubertret, M. Calame, A.J. Libchaber, Single-mismatch detection using gold-quenched fluorescent oligonucleotides. *Nat. Biotechnol.* **19**, 365–370 (2001). <https://doi.org/10.1038/86762>
 39. H. Tang, N. Zhang, Z. Chen et al., Probing hydroxyl radicals and their imaging in living cells by use of FAM-DNA-Au nanoparticles. *Chem. Eur. J.* **14**, 522–528 (2008). <https://doi.org/10.1002/chem.200700455>
 40. S.J. Hurst, A.K.R. Lytton-Jean, C.A. Mirkin, Maximizing DNA loading on a range of gold nanoparticle sizes. *Anal. Chem.* **78**, 8313–8318 (2006). <https://doi.org/10.1021/ac0613582>
 41. Z.B. Wen, W.B. Liang, Y. Zhuo et al., An efficient target-intermediate recycling amplification strategy for ultrasensitive fluorescence assay of intracellular lead ions. *Chem. Commun.* **53**, 7525–7528 (2017). <https://doi.org/10.1039/c7cc04104g>
 42. W. Zhou, W. Liang, D. Li et al., Dual-color encoded DNzyme nanostructures for multiplexed detection of intracellular metal ions in living cells. *Biosens. Bioelectron.* **85**, 573–579 (2016). <https://doi.org/10.1016/j.bios.2016.05.058>
 43. C. Xiong, W. Liang, H. Wang et al., In situ electro-polymerization of nitrogen doped carbon dots and their application in an electrochemiluminescence biosensor for the detection of intracellular lead ions. *Chem. Commun.* **52**, 5589–5592 (2016). <https://doi.org/10.1039/c6cc01078d>